Supplementary Material (ESI) for Journal of Materials Chemistry

Towards understanding palladium doping of carbon supports: A first-principles molecular dynamics investigation

Samir H. Mushrif [a], Alejandro D. Rey [a], Gilles H. Peslherbe [b,*]

[a] Department of Chemical Engineering, McGill University, Montréal, QC, H3A2B2, Canada

[b] Center for Research in Molecular Modeling and Department of Chemistry and Biochemistry, Concordia University, Montréal, QC, H4B1R6, Canada

I. Computational Details

Simulation system set-up

A cubic simulation cell 13Å wide on each side with periodic boundary conditions was used. The chemical composition of the cell is shown in Figure S1: the cell contains 5 chrysene molecules and 2 palladium (II) acetylacetonates (*cf.* Figure S1a), yielding a density of 1.35 g/cc. The distance between individual molecules was fixed arbitrarily, but a topological analysis of the electron localization function (ELF) of the initial system (following geometry optimization) was performed to make sure that there were no "pre-existing" intermolecular interactions within the simulation cell (*cf.* Figure S1b). Chrysene was chosen as a model polyaromatic hydrocarbon in this work because, in the investigation of the effects of metal precursor–carbon chemistry on the microstructure of palladium-loaded carbon fibers by Edie and coworkers,[1] chrysene was shown to be one of the major components of the pitch used to prepare the carbon support. Furthermore, when palladium (II) acetylacetonate was mixed with the pitch, a significant decrease of the concentration of chrysene in the pitch was observed, suggesting that palladium (II) acetylacetonate is chemically interacting with the pitch chrysene molecules at the initial mixing stage. Based on this observation, it was suggested that this palladium complex–aromatic carbon chemistry governs the microstructure and the chemical composition of the resulting fibers. However, the exact nature of the interaction between palladium (II) acetylacetonate and chrysene remained unclear.

The molecular dynamics (MD) simulations were performed at 500 K, the temperature at which palladium (II) acetylacetonate is mixed with the carbon-support-precursor pitch[2] in the synthesis of palladium-doped carbon supports, especially carbon fibers. This temperature is lower than that at which palladium (II) acetylacetonate thermally decomposes (by itself), and it is within ±50 K of the temperature at which the prepared and preshaped carbon support is heated (in an inert atmosphere and in the presence of H_2 for reduction of palladium) when contacted with a palladium precursor.[3]

The simulation system was limited to two palladium (II) acetylacetonate molecules due to computational cost constraints and multiplicity issues. A multiplicity of 5 was chosen, as it was found to be the lowest-energy spin state of a system made up of two palladium cations. Increasing the number of palladium (II) acetylacetonate molecules would result in a factorial increase of the possible multiplicities, in turn increasing the number of computations and possibly leading to convergence problems.

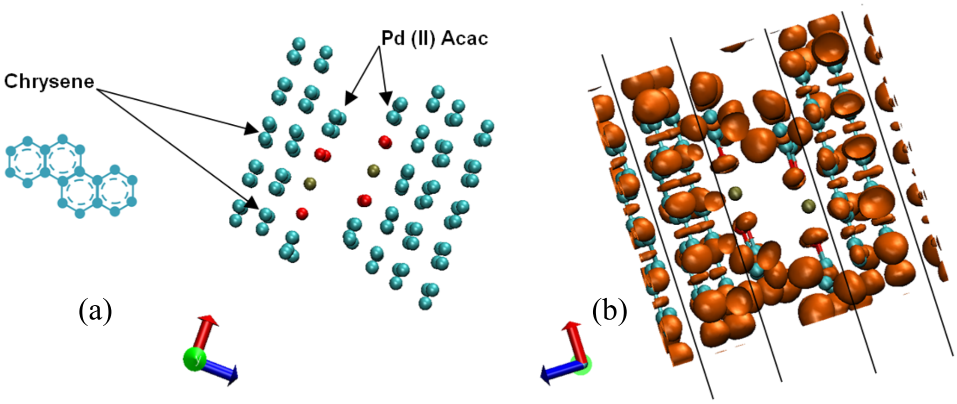

Figure S1: *(a) The simulation cell containing the chrysene molecules and palladium (II) acetylacetonates and (b) ELF isosurfaces at an isovalue of 0.8 showing no "pre-existing" intermolecular interactions.*

Computational Methods:

Calculations were performed using the CPMD software, version 3.11.1,[4] which provides an implementation of the first-principles Car-Parrinello molecular dynamics (CPMD) scheme. The first-principles calculations were performed using the planewave pseudopotential implementation of the Kohn-Sham formulation of density-functional theory. The Troullier-Martins pseudopotentials[5] with the Perdew-Burke-Ernzerhof generalized gradient approximation,[6] which have been validated in our previous work,[7] were used. Only the Γ-point was used for integration over the Brillouin zone in reciprocal space. The planewave energy cut-off for the pseudopotential was determined by inspection of the variation of the energy of the system with energy cut-off. A cut-off of 100 Ryd. produced a converged energy, and was thus used thereafter. To check for spin contamination in our calculations, even though it is in principle not an issue in density-functional theory, $\langle S^2 \rangle$ was estimated using the procedure given by Wang et al.[8] (as CPMD calculates the total integrated value of the spin density and not $\langle S^2 \rangle$). Since the estimated $\langle S^2 \rangle$ value (6.35) was found to be within 10% of the exact value (6.00) for a system with quintet multiplicity, spin contamination appears to be negligible in our calculations.

Temperature control was achieved using the Nosé-Hoover thermostat. The frequency for the ionic thermostat was 1800 cm^{-1} (characteristic of a C–C bond vibration frequency) and that for the electron thermostat was 10000 cm^{-1}. The fictitious electron mass was taken as 600 a.u. Short MD runs were performed without the thermostat to obtain an approximate value around which the electronic kinetic energy oscillates; a value of the electronic kinetic energy of 0.14 a.u. was chosen and used in further simulations. The MD time step used in the simulation was 0.0964 fs. The system was first equilibrated for 0.25 ps (to have the Kohn-Sham energy oscillate around a mean value) and then a production run of 7 ps was performed. Figure S2 shows the variation of the fictitious electronic kinetic energy of the system during the CPMD run; the fictitious electronic kinetic energy oscillates around the mean value of 0.14 a.u., confirming that the electrons do not "heat up" in the presence of the "hot" nuclei and the system remains in the Born-Oppenheimer ground state. A Born-Oppenheimer molecular dynamics (BOMD) simulation of 1 ps, with a time step of 0.482 fs, was also performed for the equilibrated system, and excellent agreement between the CPMD and BOMD trajectory results was found. Due to the high computational cost of BOMD simulations for this system (36000 CPU-hours for a simulation over 1 ps on a Dell 1425SC cluster of 576 nodes with Infiniband 4X interconnect), the CPMD scheme was used thereafter for longer simulations (computational cost of 7700 CPU-hours for a simulation over 1 ps).

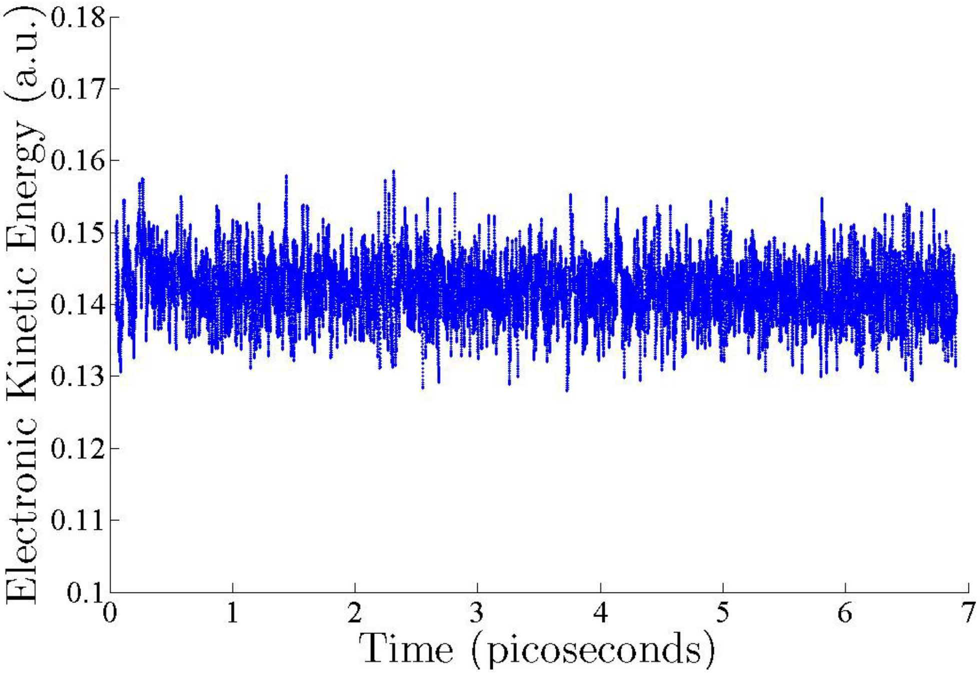

Figure S2: *Fictitious electronic kinetic energy vs. time during the CPMD production run.*

The electron localization function (ELF), introduced by Becke and Edgecombe[9] was used to characterize the nature of the interactions between atoms and molecules along the MD trajectory. Silvi and Savin[10] proposed a topological analysis of the ELF to classify chemical bonds as covalent or ionic, and to characterize multiple bonds. Inspection of localization domains, the spatial regions bounded by a closed ELF isosurface, also provides insight into the electronic structure. At low values of the ELF, there is only one localization domain, containing all the attractors (local maxima). As the ELF value is increased, the localization domain splits into a number of irreducible and reducible domains, containing one and multiple attractors, respectively, until all domains become irreducible, giving rise to distinguishable valence basins. The synaptic order of a valence basin, i.e. the number of atomic core basins in contact with the valence basin, can be used to characterize the chemical interaction as electron-sharing or non electron-sharing.[11] The hierarchy of bifurcations of the valence basins with increasing ELF isovalue can also be related to the relative electronegativities of atoms in molecules, and hence can be used to identify the most electronegative atom in a molecule.[12] Finally, Kohout and Savin[13] also provided a method to calculate the ELF separately for each spin density. Spin-dependent ELF calculations provide information about the localization of unpaired electrons (e.g. the two unpaired electrons of palladium in our simulation system).

II. Additional Results

ELF analysis of palladium-oxygen interactions

The variation of the palladium–oxygen bond distances in the palladium (II) acetylacetonate along the MD trajectory shows that palladium remains associated with one of the acetylacetonate moiety and detaches from the other. The ELF topology of the decomposed palladium (II) acetylacetonate was also compared to that of an intact palladium (II) acetylacetonate. Figure S3 shows *contour plots* (these are not actual contour plots, but were constructed from ELF isosurfaces corresponding to different isovalues ranging from 0.2 to 1, sliced through the plane of palladium acetylacetonate) of the ELF for both palladium (II) acetylacetonates. The ELF results support the earlier conclusions that palladium detaches from one acetylacetonate ligand and remains associated with the other. The position of the lone pairs of the oxygens bonded to palladium is similar to that for an intact palladium (II) acetylacetonate, while that for the oxygens not having a bonded interaction with palladium reveal completely different.

III. Additional Relevant Information (Experiments and Simulations)

As mentioned in the manuscript, palladium is incorporated on a carbon support for a variety of reasons, including catalysis and hydrogen storage. The conventional method of palladium doping is impregnation of the palladium precursor on the carbon support, followed by hydrogen reduction. The chemistry of palladium precursors and carbon affects the electronic structure of the active sites (since it depends on the palladium-carbon interactions), the number of active sites (since a weak palladium-carbon interaction leads to sintering of palladium particles) and the microstructure of the carbon support (uncontrolled dispersion of palladium particles may clog the desired pores in the support).

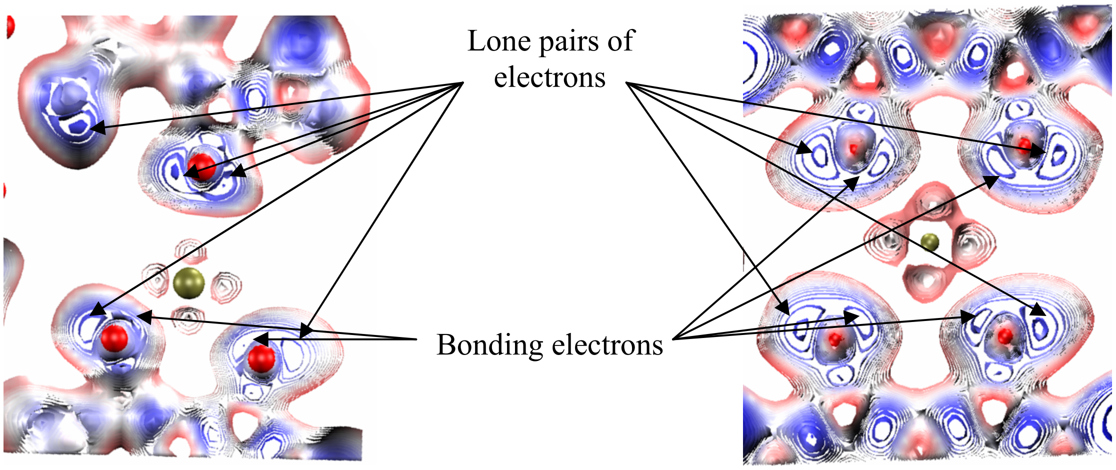

(a) **(b)**

Figure S3: *ELF contour plots (a) for palladium (II) acetylacetonate decomposed in the presence of chrysene molecule and (b) for an intact palladium (II) acetylacetonate molecule.*

The other, more recent, method for palladium doping is to mix the palladium precursor with the carbon support precursor before the preparation of the carbon support. After mixing, the carbon material, containing the palladium precursor, undergoes carbonization and activation at temperatures as high as 1250 K.[2] Analysing the effect of palladium precursor–carbon chemistry on the (i) electronic structure of active sites, (ii) the dispersion of palladium particles and (iii) the pore structure of the carbon support is relatively more difficult in this case. Though there is a significant body of literature related to both types of carbon-supported palladium materials, there are very few investigations related to the chemistry implicated in the synthesis of these materials. In this section, additional experimental and simulation results that support our findings are reviewed.

(i) Tribolet et al.[14] prepared palladium-loaded carbon nanofibers (grown on sintered metal fibers) and active carbons by the adsorption of a palladium precursor on both carbon supports, and heating the samples to 400 K in the presence of He and H_2. They observed smaller palladium particles and better dispersion of palladium in the case of carbon nanofibers, and concluded that there exists a strong palladium-carbon interaction, stronger than a cation-π interaction that prevents the sintering of palladium particles.

(ii) Kim et al.[15] prepared mono-dispersed palladium nanoparticles using palladium (II) acetylacetonate and trioctylphosphine, and showed using FT-IR spectroscopy that palladium (II) acetylacetonate decomposes as the acetylacetonate ligands separate from the palladium center.

(iii) Simulation studies[16,17] of palladium atoms sandwiched between polyaromatic hydrocarbons have shown that palladium does not tend to locate over the centre of the carbon ring, but rather attaches to the peripheral carbon atoms of the aromatic ring. However, no simulation studies of the interaction of palladium precursors with aromatic carbons have been reported, to the best of our knowledge.

(iv) Tamai et al.[18] were pioneers in mixing palladium (II) acetylacetonate with a petroleum pitch to prepare palladium-loaded pitch-based carbon fibers for 1-hexene hydrogenation catalysis. They noticed the appearance of a palladium peak in the X-Ray diffraction profiles at temperatures higher than 900 K. This suggests that though the decomposition of palladium (II) acetylacetonate is initiated after mixing with the carbon precursor, palladium does not get completely separated from its precursor at 500 K, so as to form palladium particles.

(v) Edie et al.[1,19,20] have performed extensive studies in the field of palladium-loaded pitch-based activated carbon fibers. Palladium (II) acetylacetonate was used as the palladium precursor and it was mixed with the aromatic pitch at 500 K. This work provided substantial evidence of the presence of a chemical interaction between palladium (II) acetylacetonate and the pitch aromatic carbons at this temperature. Five major polyaromatic hydrocarbons were identified in the precursor pitch (including chrysene) using gas chromatography–mass spectrometry, and the concentration of all the polyaromatic hydrocarbons in the pitch was observed to decrease by up to 20 % following mixing. Palladium was also hypothesized to separate from the acetylacetonate ligands at this stage and attach to the hydrocarbons.

(vi) Wu et al.[21] studied the same material as in (v), and reported reduced distances between the parallel stacks of polyaromatic carbons in palladium (II) acetylacetonate-doped activated carbon fibers, thereby indicating an enhanced interaction and cross-linking between the aromatic carbons in the palladium-containing carbon support.

(vii) Recently, Okabe et al.[22] prepared palladium-loaded molecular sieving carbons (MSC) by mixing polyamic acid with palladium (II) acetylacetonate. The mixture was then heated to 573 K and then carbonized at temperatures as high as 1273 K. A thermogravimetric analysis indicated that palladium (II) acetylacetonate decomposes at 473 K in the presence of polyamic acid during the mixing stage. However, in the X-Ray diffraction analysis, no peak was observed for pure palladium till the carbonization temperature reached 873 K. The simulation studies reported in this paper also demonstrate the decomposition of palladium (II) acetylacetonate in the presence of chrysene molecules at 500 K but the formation of pure palladium is not observed.

(viii) The bonding of palladium with the polyaromatic hydrocarbons (PAHs) found in this work in the initial stage of doping might prevent the sintering of palladium during the later carbonization and activation steps, and the covalent cross-linking of PAHs could provide additional stability to the metal-doped carbon fibers, thereby preventing the formation of larger mesopores and macropores, in agreement with experimental observations. The mechanism of interaction of palladium (II) acetylacetonate with the PAHs unveiled in this Communication most likely also applies to acetylacetonate complexes with other metals (Cu, Pt, Ni, etc.) which are often used as precursors for metal doping of carbon supports. The metal-ligand covalency in these complexes was found to increase with the atomic number of the metal,[23] and increased metal-ligand covalency could result in decrease or loss of conjugation in the attached ligand electronic structure, which in turn could result in increased reactivity of the (less stable) ligand towards the PAHs. This analysis is consistent with experimental findings: upon mixing of the metal complex with PAHs at 500 K, a larger decrease in the concentration of the PAHs was observed for Pd, compared to Co,[1] indicating a larger extent of reaction of the PAHs with Pd, the metal with highest atomic number. A larger extent of reaction between the metal complex and the

PAHs will also result in increased covalent cross-linking of PAHs, providing additional stability of the fibers, and thereby preventing the formation of larger mesopores and macropores. Again, this is consistent with the experimental observation that the activation time for Pd-doped fibers is almost 10 times longer than that for Co-doped fibers, and that the average pore size of Pd-doped fibers is smaller than that of Co-doped fibers. Finally, the higher propensity of Pd to covalently bind to ligands may also explain the smaller extent of sintering of Pd particles during the fiber preparation, compared to that of Co particles, as the Pd particles are more likely to interact with the PAHs following metal-ligand complex dissociation (as found in this work) than with each other.

IV. References

(1) Basova, Y. V.; Edie, D. D. *Carbon* **2004**, *42*, 2748-2751.

(2) Lee, Y. S.; Basova, Y. V.; Edie, D. D.; Reid, L. K.; Newcombe, S. R.; Ryu, S. K. *Carbon* **2003**, *41*, 2573-2584.

(3) Krishnankutty, N.; Li, J.; Vannice, M. A. *Applied Catalysis a-General* **1998**, *173*, 137-144.

(4) In *CPMD Copyright IBM Corp. 1990-2006, Copyright MPI für Festkörperforschung Stuttgart 1997-2001.*

(5) Troullier, N.; Martins, J. L. *Physical Review B* **1991**, *43*, 1993-2006.

(6) Perdew, J. P.; Burke, K.; Ernzerhof, M. *Physical Review Letters* **1996**, *77*, 3865-3868.

(7) Mushrif, S. H.; Rey, A. D.; Peslherbe, G. H. *Chemical Physics Letters* **2008**, *465*, 63-66.

(8) Wang, J. H.; Becke, A. D.; Smith, V. H. *Journal of Chemical Physics* **1995**, *102*, 3477-3480.

(9) Becke, A. D.; Edgecombe, K. E. *Journal of Chemical Physics* **1990**, *92*, 5397-5403.

(10) Silvi, B.; Savin, A. *Nature* **1994**, *371*, 683-686.

(11) Silvi, B.; Fourre, I.; Alikhani, M. E. *Monatshefte Fur Chemie* **2005**, *136*, 855-879.

(12) Fuster, F.; Sevin, A.; Silvi, B. *Journal of Computational Chemistry* **2000**, *21*, 509-514.

(13) Kohout, M.; Savin, A. *International Journal of Quantum Chemistry* **1996**, *60*, 875-882.

(14) Tribolet, P.; Kiwi-Minsker, L. *Catalysis Today* **2005**, *105*, 337-343.

(15) Kim, S. W.; Park, J.; Jang, Y.; Chung, Y.; Hwang, S.; Hyeon, T.; Kim, Y. W. *Nano Letters* **2003**, *3*, 1289-1291.

(16) Philpott, M. R.; Kawazoe, Y. *Chemical Physics* **2007**, *337*, 55-67.

(17) Philpott, M. R.; Kawazoe, Y. *Chemical Physics* **2008**, *348*, 69-82.

(18) Tamai, H.; Kataoka, Y.; Nishiyama, F.; Yasuda, H. *Carbon* **2000**, *38*, 899-906.

(19) Basova, Y. V.; Edie, D. D.; Badheka, P. Y.; Bellam, H. C. *Carbon* **2005**, *43*, 1533-1545.

(20) Basova, Y. V.; Edie, D. D.; Lee, Y. S.; Reid, L. K.; Ryu, S. K. *Carbon* **2004**, *42*, 485-495.

(21) Wu, X.; Gallego, N. C.; Contescu, C. I.; Tekinalp, H.; Bhat, V. V.; Baker, F. S.; Thies, M. C. *Carbon* **2008**, *46*, 54-61.

(22) Okabe, H.; Takagi, H.; Hatori, H.; Suzuki, A.; Terai, T. *Materials Science and Engineering B-Advanced Functional Solid-State Materials* **2008**, *148*, 253-256.

(23) Lewis, F. D.; Salvi, G. D.; kanis, D. R.; Ratner, M. A. *Inorganic Chemistry* **1993**, 32, 1251-1258.